

# Field-induced charge transport at the surface of pentacene single crystals: a method to study charge dynamics of 2D electron systems in organic crystals

J. Takeya<sup>1,2,\*</sup>, C. Goldmann<sup>1</sup>, S. Haas<sup>1</sup>, K. P. Pernstich<sup>1</sup>, B. Ketterer<sup>3</sup>, and B. Batlogg<sup>1</sup>

<sup>1</sup>*Laboratory for Solid State Physics ETH, CH-8093 Zürich, Switzerland*

<sup>2</sup>*CRIEPI, 2-11-1, Iwado-kita, Komae, Tokyo 201-8511, Japan and*

<sup>3</sup>*Laboratory for Micro- and Nanotechnology PSI, CH-5232 Villigen, Switzerland*

(Dated: November 19, 2018)

## Abstract

A method has been developed to inject *mobile* charges at the surface of organic molecular crystals, and the DC transport of field-induced holes has been measured at the surface of pentacene single crystals. To minimize damage to the soft and fragile surface, the crystals are attached to a pre-fabricated substrate which incorporates a gate dielectric (SiO<sub>2</sub>) and four probe pads. The surface mobility of the pentacene crystals ranges from 0.1 to 0.5 cm<sup>2</sup>/Vs and is nearly temperature-independent above  $\sim 150$  K, while it becomes thermally activated at lower temperatures when the induced charges become localized. Ruling out the influence of electric contacts and crystal grain boundaries, the results contribute to the microscopic understanding of trapping and detrapping mechanisms in organic molecular crystals.

PACS numbers:

Keywords: field-effect device, organic molecular crystals, pentacene, charge mobility, hole mobility, temperature dependence, measurement method

---

\*Electronic address: takeya@criepi.denken.or.jp

Transport of field-induced charge in crystals of aromatic molecules is of interest in both technological and academic contexts. On one hand, organic field-effect transistors (OFETs) provide key components in “plastic electronics” such as active matrix flexible displays, where OFETs are used as pixel control devices [1]. On the other hand, though a wide variety of organic materials have been studied, relatively little is known about the details of microscopic intermolecular-transport dynamics, especially trapping and detrapping mechanisms, even for simple molecules such as polyacenes [2]. For example, a frequently addressed question is how the field-effect mobility of OTFTs relates to molecular order [3, 4]. An experimental difficulty has been that intrinsic transport properties are masked by structural imperfections and the device performance is limited by inefficient carrier injection because most of the devices reported on to date involve polycrystalline thin films. Therefore, it is desirable to measure field-induced transport in single crystals, applying a method which avoids disturbing the crystal surface as much as possible. Of further scientific interest is a possible electronic phase transition to intriguing states in such van-der-Waals crystals with moderate orbital overlaps between adjacent molecules, when the carrier density is high enough; ordered electronic ground states have been demonstrated in the form of superconductivity in doped fullerenes and complex charge-ordered states in charge-transfer compounds [5, 6].

Using the metal-oxide-semiconductor (MOS) structure, one can continuously tune the amount of charge confined to a two-dimensional layer near the surface, so that the evolution of the field-induced charge transport can be systematically studied. However, the main difficulty lies in preventing the injected charge from being trapped by interface states. Although the surface of van-der-Waals crystals is free from dangling bonds and can be highly ordered, the surface can be damaged when depositing a gate oxide film. In this report, we present a general method of fabricating molecular single crystal MOS structures which avoids this problem: a set of probing electrodes is defined on top of a thermally oxidized silicon wafer which provides a gate insulator and gate electrodes. A separately grown pentacene crystal is then attached on the substrate, minimizing the damage to the crystal surface. In such devices, the electrically induced charge is mobile due to the good interface quality. A crossover from thermally activated transport to temperature-independent conduction is observed in four-terminal measurements, excluding parasitic effects from the source and drain contacts.

Figure 1(a) schematically shows the fabrication process of the crystal-based MOS structure. We use a heavily doped n-type silicon wafer ( $p \simeq 0.016 \Omega \text{ cm}$  @ RT) as a substrate.

The wafer is cleaned in a solution of sulfuric acid and hydrogen peroxide @ 80 °C, then oxidized in dry O<sub>2</sub> @ 1150 °C to grow a high-quality gate insulator. The surface roughness (as measured by AFM) over the typical size of the device ( $\sim 0.1$  mm) is less than 1 nm, and the oxide has a thickness of 0.5-1  $\mu\text{m}$ . Probing electrodes (1 nm Cr for adhesion and 9 nm Au) for four-terminal measurements are defined by electron-beam lithography. The distance between the two voltage-probing pads is approx. 5  $\mu\text{m}$ . This small separation reduces the likelihood of having macroscopic defects such as molecular steps in the channel of the device.

Next, the SiO<sub>2</sub> is coated with a self-assembled monolayer of octadecyltrichlorosilane (OTS) with a thickness of  $\sim 3$  nm. It is found that the monolayer reduces trapped charges at the interface [7]. To improve the electrical contact between the gold pads and the molecular crystal, the substrate is treated in a solution of 10 mM nitrobenzenethiol in ethanol. The thiol bonds to the gold surface, and the nitro group dopes holes into the surface of the crystal because of its large electron affinity. The treatment significantly reduces the contact resistance (approx. by a factor of 10 at room temperature and much more at low  $T$ ), which is crucial for the low-temperature four-terminal measurement. After the surface treatments, the conductivity between the probe electrodes remains immeasurably small when a gate voltage is applied, indicating that the OTS monolayer is highly insulating.

Pentacene single crystals are grown separately by the physical vapor transport technique [8]. Starting from commercial powders of the same material (Fluka), the growth is repeated three times to purify the crystals. For a good adhesion to the substrate, it is preferable to choose a thin transparent crystal, with typical thickness of 2-5  $\mu\text{m}$ . Since the probing electrodes are visible through the crystal, the crystal can be located so that the most homogeneous part is placed between the electrodes. Electrostatic force ensures a strong adhesion of the crystal to the substrate. Alternatively, adhesion can be imposed by applying a gate voltage. A picture of a typical sample is shown in Fig. 1(b), where no grain boundary is visible in the channel.

On these devices, four-terminal measurements have been performed using four Keithley 6517A electrometers/high-impedance meters. Figure 1(c) shows the corresponding circuit diagram. One of the electrometers applies the voltage  $V_{GD}$  and monitors the leakage current  $I_G$  through the dielectric, another applies the source-drain voltage and measures the current  $I_S$  in the sample, and the others measure the difference in potential between the two intermediate electrodes and the drain electrode ( $V_1$  and  $V_2$ ). The sheet conductivity  $\sigma_{\square}$  of

the channel is given by  $I_S/(V_2 - V_1) \cdot l/w$ , regardless of the voltage drops across the source and drain contacts ( $l$  and  $w$  are the distance between the two intermediate electrodes and the width of the channel, respectively). The drain electrode is set common for the  $V_{GD}$  and  $V_{SD}$  application (in contrary to the standard connection of MOS transistors). Since only the “linear regime” of the channel  $I - V$  characteristics is of interest for the four-terminal method, the polarity of  $V_{SD}$  is chosen opposite to the polarity of  $V_{GD}$  to avoid the “pinch-off” saturation in  $I_S$ . For convenience, we additionally define  $V_G \equiv V_{GD} - (V_1 + V_2)/2$ , which represents an effective gate voltage with respect to the central part of the channel where the sheet conductivity is measured.

The distance between the two current-injecting electrodes is approximately 10-15 times longer than the width of these electrodes, so that the most of the current flows through the field-accumulated channel between them. In order to estimate the influence of the current flowing via the voltage electrodes, we also performed measurement using the circuitry illustrated in Figure 1(d); using a guarding function with a high input impedance (a voltage follower) of the Keithley 6517A, a set of two voltage pads (no. 1 and 3 in the figure) is held at the same potential level, so that no current flows between these pads. The channel conductivity in the guarded circuit was measured to be  $\sim 6\%$  smaller than in the unguarded circuit.

A drawback of the guarded measurement is its slower response, as it is necessary to minimize the redistribution of trap centers at the interface in response to high electric fields applied over a long time. As reported by Schoonveld *et al.* for pentacene thin-film devices on  $\text{SiO}_2$  [9], localized charges randomly distributed in pentacene and/or the  $\text{SiO}_2$  can slowly move towards the interface in response to a relatively high gate voltage. Therefore, the distribution of the hole-trapping centers changes and the measured values of the field-induced current are not exactly reproduced after prolonged influence of  $V_G$ . The redistribution is faster at higher temperatures and at higher gate voltages. In order to minimize the effect of this charge relaxation, we swept  $V_{GD}$  at a fixed  $V_{SD}$  as quickly as  $\sim 30$  s per sweep, using the unguarded circuitry, minimizing hysteresis effects. Moreover,  $I_{SD}$  thus measured is reproduced after a set of measurements at different temperatures, ensuring that the relaxation effect is negligible in the measurements.

In Fig. 2(a) and (b),  $I_S$  at fixed values of  $V_{SD}$  is plotted for two temperatures as a function of  $V_G$ . The source current in the pentacene single crystal substantially increases

due to hole injection by the negative  $V_G$ . On the other hand, no enhancement of  $I_S$  is detected with positive gate voltage. The influence of leakage current through the dielectric  $I_G$  is negligibly small (less than 0.1% of  $I_S$ ). In Fig. 2(c),  $\sigma_{\square}$  is plotted against  $V_G$ , where 6% is subtracted from the result of the unguarded measurement. The curves for different values of  $V_{SD}$  are close to each other, indicating a nearly ohmic current-voltage relationship for the field-induced conductivity at the surface [10]. The observed curvature resembles that of typical organic field-effect transistors (FETs) and is consistent with a standard model: the injected charge is trapped until  $V_G$  reaches a threshold voltage  $V_{th}$ , and the amount of trap-free charge is given by  $p_{free}e = \epsilon\epsilon_0(V_G - V_{th})/d$ . In reality, the crossover is usually gradual [11, 12]. As the surface mobility  $\mu$  equals to  $\sigma_{\square}/(p_{free}e)$ , where  $e$  is the charge of an electron,  $\mu$  for this sample can be estimated from the slope to be  $\sim 0.1 \text{ cm}^2/\text{Vs}$  with an uncertainty of 15-20%.

Figure 3(a) presents the  $\sigma_{\square}$ - $V_G$  curves at different temperatures from 160 K to 260 K. While the temperature dependence is obvious in the low  $V_G$  region, the maximum slope at high  $V_G$  does not differ much as a function of temperature. For each temperature, the mobility is estimated from this maximum slope and is plotted in Fig. 3(b). The results for two more crystals are also shown. The mobility values range from 0.1 to 0.5  $\text{cm}^2/\text{Vs}$ , with no apparent temperature dependence. These mobilities are comparable to typical room temperature bulk values measured in naphthalene by the time-of-flight method [13], though an ultraclean crystal can show a rapid increase in  $\mu(T)$  upon cooling [14, 15]. The mobility values of our devices are also comparable to those of high-quality pentacene thin-film FETs, though somewhat smaller than the best MOS device (1.5  $\text{cm}^2/\text{Vs}$ ) [16]. (More recently, a mobility of 3  $\text{cm}^2/\text{Vs}$  was reported for pentacene OTFTs with a polymeric dielectric [17].) The absence of a temperature dependence is reported for the high-mobility devices of Ref. 16 as well; however, possible contributions from grain boundaries and electric contacts limited further discussion of the origin of the  $T$  independence. Since it is not likely that such extrinsic mechanisms dominate  $\mu(T)$  in our four-terminal measurements of single crystals, the nearly temperature independent  $\mu(T)$  (at least from  $\sim 150$  K to near room temperature) appears to be an intrinsic property of the surface of the pentacene single crystals in this study, motivating us to investigate the fundamental inter-molecular charge dynamics more quantitatively.

The nearly  $T$ -independent feature is inconsistent with usual hopping models which predict

strong  $T$  dependence as  $\sim T^{-m} \exp(-\Delta/k_B T)$ . A difficulty arises in the band picture as well because a naive estimation of the mean free path  $\ell$  results in a value shorter than the distance between adjacent molecules  $a \sim 5 \text{ \AA}$ ; assuming the free-electron approximation  $\mu = e\tau/m^* = e\ell/m^*\bar{v}$  ( $\tau$  and  $m^*$  are the relaxation time and the effective mass, respectively) and the 2D Boltzmann distribution of the average velocity  $\bar{v} = \sqrt{2k_B T/m^*}$ ,  $\ell/a$  is evaluated as  $\sim 0.1$ , even if  $\mu \sim 0.5 \text{ cm}^2/\text{Vs}$ ,  $T = 300 \text{ K}$ , and  $m^*$  is 1.5-5 times the free-electron mass [18] (the Fermi temperature is as low as  $\sim 40 \text{ K}$  even at  $V_G = 100 \text{ V}$ ). Allowing for polaron formation, which is common in dilute-charge systems, the nearly  $T$ -independent feature is deduced for naphthalene [19]; however, since the calculation is based on a balance between electronic parameters (such as band width) and phononic parameters, the applicability to the case of pentacene crystals would need to be further explored. The combination of a short  $\ell$  and an almost  $T$ -independent conductivity is reminiscent of an almost  $T$  independent inter-layer charge transport near room temperature in a high- $T_c$  cuprate. There, metallic planes are stacked in a sub-nanometer distance. It is argued that direct tunneling between the adjacent planes dominates the inter-layer transport in such systems [20].

In order to gain more insight into the transport mechanism of the field-induced charges, we extended the measurements on Sample C to lower temperatures, where the influence of the traps remains visible even at the highest applied gate voltage. The field-induced conductivity at fixed gate voltages  $\sigma_{\square}^{FET}(V_G) (\equiv \sigma_{\square}(V_G) - \sigma_{\square}(0))$  is plotted in Fig. 4 as a function of temperature. The amount of induced charge  $p$  shown in the figure is calculated from  $V_G$ . The conductivity is nearly temperature independent above  $\sim 150 \text{ K}$  reflecting  $\mu(T)$  shown in Fig. 3(b), and rapidly diminishes with an activation-like temperature dependence upon further cooling. The ‘‘activation energy’’  $\Delta$ , estimated from the slope of the  $\log \sigma_{\square}^{FET} - 1/T$  plot, is comparable to or less than room temperature and slightly decreases with increasing  $V_G$  (inset Fig. 4). The observation on the low- $T$  side is similar to recent results by Schoonveld *et al.* on a large-grain thin-film FET [21], where the channel is restricted to a single domain and the influence of the contacts is analytically subtracted. The value of  $\Delta$  in ref. 21 is similar to the ones we report here, and smaller at higher  $V_G$ , though the room temperature conductivity (and mobility) is more than one order smaller than that of Sample C. Therefore, the observed temperature and  $V_G$  dependence may reflect the generic behavior of the the conductivity at the surface of organic crystals influenced by shallow trap potentials. The dependence of  $\Delta$  on  $V_G$  can be rationalized assuming a distribution of the trap levels as in

amorphous semiconductors [22], because an increasing number of injected holes lowers the energy necessary to activate localized holes up to the “mobility edge”. However, one would question the reason of such qualitative similarity between the transport in single crystals and in amorphous systems, taking into consideration the extreme difference in the extent of the molecular order. In this sense, the microscopic mechanism causing the localization still remains to be elucidated in organic field-effect transistors.

An intriguing mechanism is proposed in ref. 21 for the charge localization; random charges located at defects near the interface induce “offset charges” in the molecules, so that the field-induced holes must hop from molecule to molecule feeling a random potential via the charging energy due to the Coulomb interaction. A noteworthy prediction is that a  $T$ -independent tunneling probability governs the inter-molecular charge transport when the above localization mechanism becomes less significant because of either high temperature or high average hopping rate between the molecules. This may provide an interpretation of an almost  $T$ -independent  $\mu$  as intrinsic to high-mobility pentacene field-effect devices. Measurements on single-crystal devices of various molecular compounds may help to elucidate the microscopic mechanism limiting the field-induced charge transport. Very recently, single-crystal measurements have indeed been successful [23, 24, 25, 26].

In summary, we have studied the transport of field-induced charge in pentacene single crystals by means of a new four-terminal method in which extrinsic contributions from grain boundaries and electric contacts are minimized. The hole mobility is comparable to the one in high-quality pentacene OTFTs. The induced sheet carrier densities are of the order from  $10^{11}$  to  $10^{12}$   $\text{cm}^{-2}$  and lead to a temperature independent conductivity above  $\sim 150$  K which correlates well with a high mobility of  $\sim 0.5$   $\text{cm}^2/\text{Vs}$ . At lower temperatures, a crossover to thermally activated transport governed by shallow traps is observed. The presented method is well suited to investigate transport in other organic crystals and to study fundamental charge transport mechanisms in the 2D electronic systems in molecular crystals.

The authors acknowledge helpful discussions with D. Gundlach, T. Hasegawa, Ch. Bergemann, K. Ensslin, Ch. Helm, S. Wehrli, M. Sigrist and R. Kleiner. We also thank K. Mattenberger, H.-P. Staub, M. Moessle, V. Oehmichen, H. Scherrer, N. Boos, S. Kicin, A. Fuhrer, and Ch. Ellenberger for technical support. This study was supported by the Swiss National Science Foundation.

- 
- [1] C. Dimitrakopoulos and P. Malenfant, *Adv. Mater.* **14**, 99 (2002).
- [2] M. Pope and C. Swenberg, *Electronic Processes in Organic Crystals and Polymers, 2nd ed.* (Oxford University Press, 1999).
- [3] D. J. Gundlach, Y. Y. Lin, T.N.Jackson, S. F. Nelson, and D. G. Schlom, *IEEE Elect. Dev. Lett.* **18**, 87 (1997).
- [4] A. Dodabalpur, L. Torsi, and H. E. Katz, *Science* **268**, 270 (1995).
- [5] M. Dresselhaus, G. Dresselhaus, and P.C.Eklund, *Science of Fullerenes and Carbon Nanotubes* (Academic Press, 1996).
- [6] T. Ishiguro, K. Yamaji, and G. Saito, *Organic Superconductors, 2nd ed.* (Springer, Berlin, 1997).
- [7] D. J. Gundlach, L.-L. Jia, and T.N.Jackson, *IEEE Electr. Dev. Lett.* **22**, 571 (2001).
- [8] C. Kloc, P. G. Simpkins, T. Siegrist, and R. A. Laudise, *J. Cryst. Growth* **182**, 416 (1997).
- [9] W. A. Schoonveld, J. Vrijmoeth, and T. M. Klapwijk, *Appl. Phys. Lett.* **73**, 3884 (1998).
- [10] *a* (a), a. Too high  $V_{SD}$  can detrapp some localized charges and may introduce nonohmicity. In this report, we restrict  $V_{SD}$  to the nearly ohmic regime to avoid complication.
- [11] G. Horovitz, M. E. Hajlaoui, and R. Hajlaoui, *J. Appl. Phys.* **87**, 4456 (2000).
- [12] G. Horovitz, *Adv. Mater.* **10**, 365 (1998).
- [13] L. B. Schein and A. R. McGie, *Phys. Rev. B* **20**, 1631 (1979).
- [14] W. Warta, R. Stehle, and N. Karl, *Appl. Phys. A* **36**, 163 (1985).
- [15] N. Karl, *in Organic Electronic Materials: conjugated polymers and low molecular weight organic solids, ed. by R. Farchioni and G. Grosso* (Springer, 2001).
- [16] S. F. Nelson, Y.-Y. Lin, D. J. Gundlach, and T. N. Jackson, *Appl. Phys. Lett.* **72**, 1854 (1998).
- [17] H. Klauk, M. Halik, U. Zschieschang, G. Schmid, W. Radlik, and W. Weber, *J. Appl. Phys.* **92**, 5259 (2002).
- [18] J. Cornil, J. P. Calbert, and J. L. Brédas, *J. Am. Chem. Soc.* **123**, 1250 (2001), rR. C. Haddon, X. Chi, M. E. Itkis, J. E. Anthony, D. L. Eaton, T. Siegrist, C. C. Mattheus, and T. T. M. Palstra, *J. Phys. Chem. B.* **106** , 8288 (2002), M. L. Tiago, J. E. Northrup, and S. G. Louie, *Phys. Rev. B* **67** , 115212 (2003).
- [19] V. M. Kenkre, J. D. Andersen, D. H. Dunlap, and C. B. Duke, *Phys. Rev. Lett.* **62**, 1165

(1989).

- [20] S. L. Cooper and K. E. Grey, in *Physical Properties of High Temperature Superconductors*, ed. by D. M. Ginsberg, vol. IV (World Scientific, 1994).
- [21] W. A. Schoonveld, J. Wildeman, D. Fichou, P. A. Bobbert, B. J. van Wees, and T. M. Klapwijk, *Nature* **404**, 977 (2000).
- [22] M. C. J. M. Vissenberg and M. Matters, *Phys. Rev. B* **57**, 12964 (1998).
- [23] V. Podzorov, V. M. Pudalov, and M. E. Gershenson, *Appl. Phys. Lett.* **82**, 1739 (2003).
- [24] V. Y. Butko, X. Chi, D. V. Lang, and A. P. Ramirez, cond-mat/0305402 (2003).
- [25] T. Hasegawa, K. Mattenberger, J. Takeya, and B. Batlogg, preprint (2003).
- [26] A. Morpurgo, private communication (2003).

Figure captions:

FIG. 1: (a) Fabrication of the field-effect device with an organic single crystal MOS structure. The crystal is attached to the substrate in the end of the fabrication process. (b) Top view of a typical sample with a pentacene single crystal. The gold electrodes are visible through the transparent crystal. (c) and (d) Circuit diagrams to measure the transport of field-induced charge by means of the four-terminal method. (d) incorporates a guarding circuit to cut the extra current path through the voltage pads.

FIG. 2: Four-probe measurement of a pentacene single crystal field-effect device. Shown is the dependence of three quantities on the gate voltage  $V_G$  (a) the source current  $I_S$  at 260 K, (b)  $I_S$  at 180 K, and (c) the channel conductivity at both temperatures. The curves in (c) are represented with the same markers as in (a) and (b) for corresponding source-drain voltages.

FIG. 3: (a) Channel conductivity vs. gate voltage at different temperatures from 160 K to 260 K. The field-effect mobility is derived from the slope of the solid lines. (b) The field-effect mobility as a function of temperature for three different pentacene single crystal devices.

FIG. 4: Main panel: The field-induced conductivity (logarithmic scale) at four different gate voltages as a function of inverse temperature (Sample C). Dashed lines are a guide to the eye to illustrate the crossover from nearly  $T$  independent to activation like  $T$  dependence. Inset: Activation energy, estimated from the slope in the low- $T$  regime, as function of estimated total hole density.

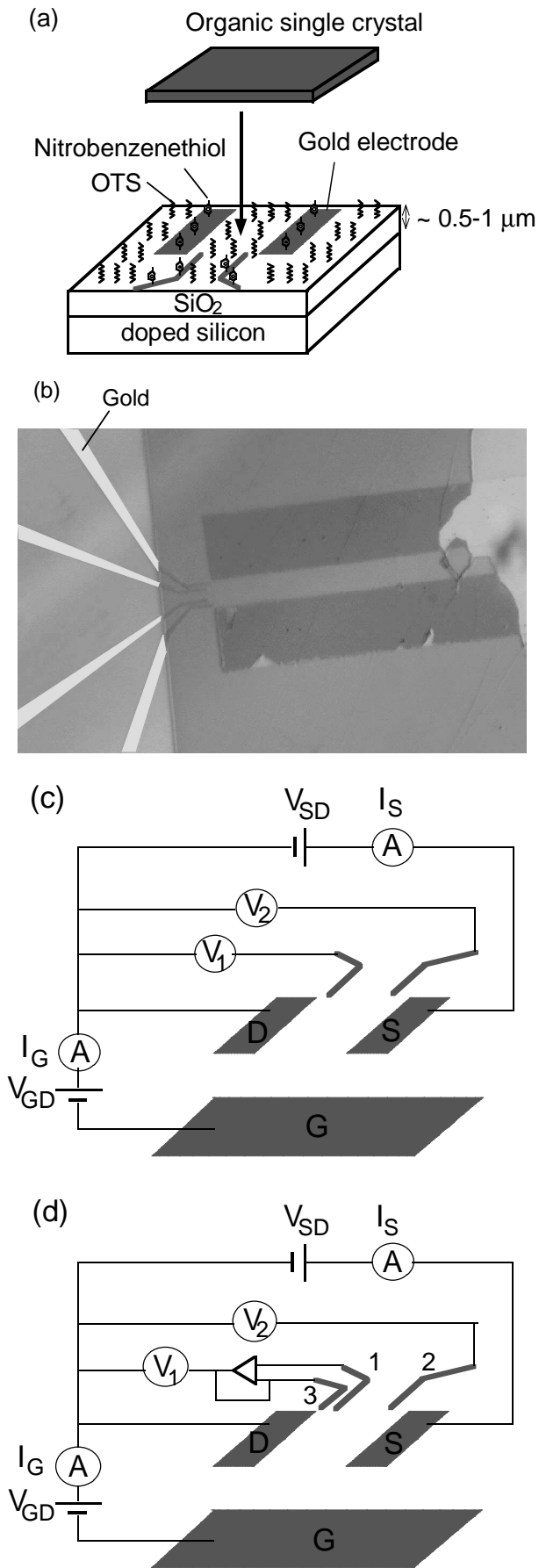


Fig. 1

J. Takeya *et al.*

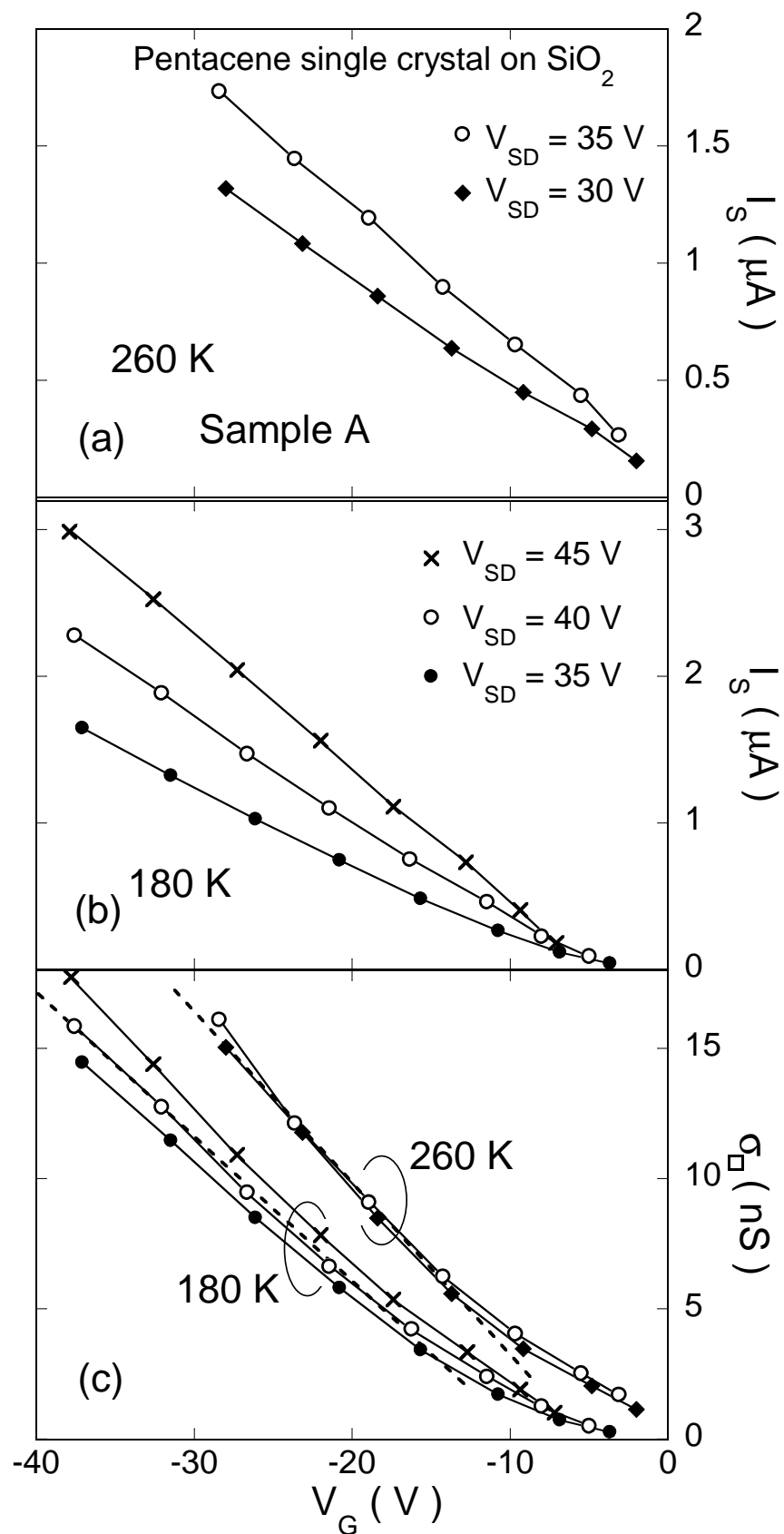


Fig. 2

J. Takeya *et al.*

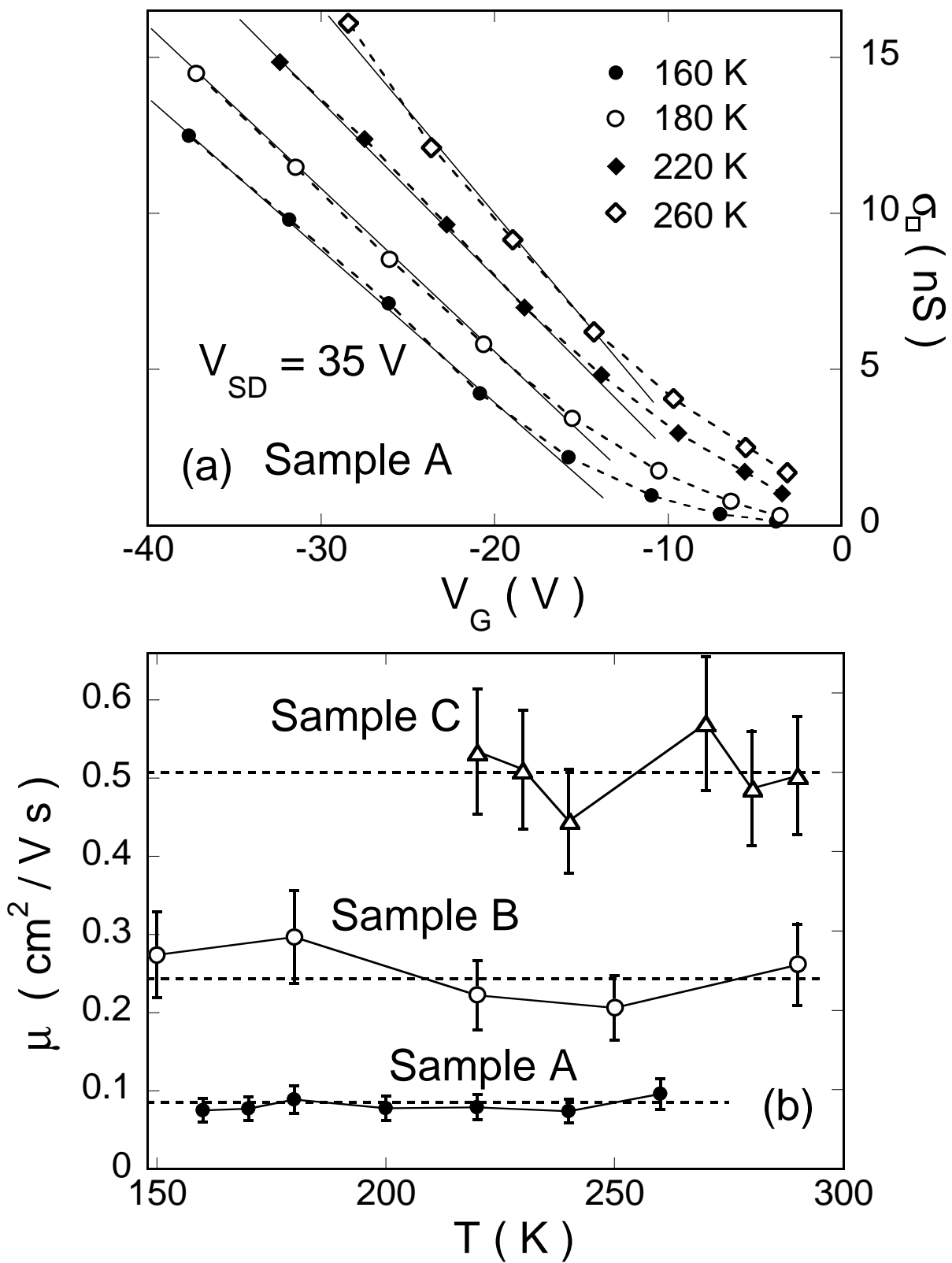


Fig. 3

J. Takeya *et al.*

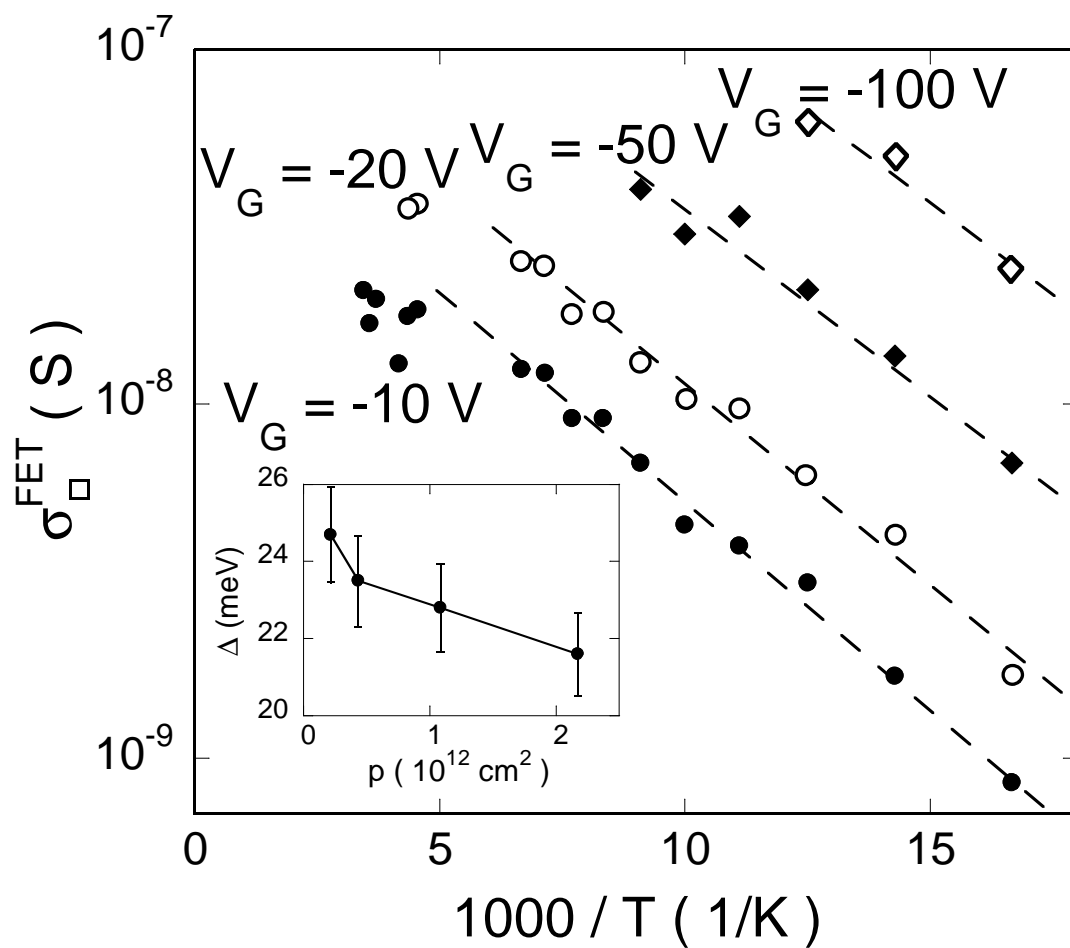


Fig. 4

J. Takeya *et al.*